

Earth and Space Science

Supporting Information for

The Post-2020 Surge in Global Atmospheric Methane Observed in Ground-based

Observations

Jennifer Wu¹, Zhao-Cheng Zeng², Sherry Luo¹, Alex J. Turner³, Debra Wunch⁴, Omaira E. García⁵, Frank Hase⁶, Rigel Kivi⁷, Hirofumi Ohyama⁸, Isamu Morino⁸, Ralf Sussmann⁹, Markus Rettinger⁹, Yao Té¹⁰, Nicholas M. Deutscher¹¹, David W.T. Griffith¹¹, Kei Shiomi¹², Cheng Liu^{13,14}, Justus Notholt¹⁵, Laura T. Iaci¹⁶, David F. Pollard¹⁷, Thornsten Warneke¹⁸, Coleen Roehl¹, Stanley P. Sander¹⁹, Yuk L. Yung¹

¹Division of Geological and Planetary Sciences, California Institute of Technology, Pasadena, California, USA, ²School of Earth and Space Sciences, Peking University, Beijing, China, ³University of Washington, ⁴Department of Physics, University of Toronto, Toronto, Canada, ⁵Izaña Atmospheric Research Center (IARC), State Meteorological Agency of Spain (AEMet), Santa Cruz de Tenerife, 38001, Spain, ⁶Karlsruhe Institute of Technology (KIT), Institute of Meteorology and Climate Research (IMKASF), 76021 Karlsruhe, Germany, ⁷Space and Earth Observation Centre, Finnish Meteorological Institute, Finland, ⁸Earth System Division, National Institute for Environmental Studies (NIES), Tsukuba, Ibaraki, Japan, ⁹Karlsruhe Institute of Technology (KIT), Institute of Meteorology and Climate Research (IMK-IFU), Garmisch-Partenkirchen, Germany, ¹⁰Sorbonne Université, CNRS, MONARIS, UMR8233, F-75005 Paris, France, ¹¹Centre for Atmospheric Chemistry, Environmental Futures Research Centre, School of Earth, Atmospheric and Life Sciences, University of Wollongong, Wollongong, NSW, Australia, ¹²Earth Observation Research Center, Japan Aerospace Exploration Agency (JAXA/EORC), ¹³Department of Precision Machinery and Precision Instrumentation, University of Science and Technology of China, Hefei 230026, China, ¹⁴Key Laboratory of Environmental Optics and Technology, Anhui Institute of Optics and Fine Mechanics, Hefei Institutes of Physical Science, Chinese Academy of Sciences, Hefei 230031, China, ¹⁵Institute of Environmental Physics, University of Bremen, ¹⁶Earth Science Division, NASA Ames Research Center, Moffett Field, California, USA, ¹⁷National Institute of Water and Atmospheric Research Ltd (NIWA), Lauder, New Zealand, ¹⁸Institute of Environmental Physics, University of Bremen, Bremen, Germany, ¹⁹Jet Propulsion Laboratory, California Institute of Technology

Contents of this file

Table S1

Figures S1 to S4

Introduction

This file contains the supplementary figures and table for The Post-2020 Surge in Global Atmospheric Methane Observed in Ground-based Observations. Table S1 contains the optimal parameters derived from the Fourier series regression of 2016-2019 data for both CLARS-FTS and the 20 TCCON sites analyzed in this study. Figures S1 to S4 contain supplementary information that is not essential for the main text flow but may be of interest to readers. Detailed explanations for each figure are provided in their respective captions.

Table S1. The optimized coefficients derived from the Fourier fitting process described in Section 2.3 along with their associated standard errors. The Fourier series equation is given by Eq. 1.

Site	α_0	$\alpha_{0,err}$	α_1	$\alpha_{1,err}$	β_1	$\beta_{1,err}$	β_2	$\beta_{2,err}$	β_3	$\beta_{3,err}$	β_4	$\beta_{4,err}$
CLARS-FTS	1789.67	5.75	0.34	0.09	3.28	1.22	-3.18	1.26	-6.37	1.22	1.23	1.23
Bremen	1792.63	6.28	0.69	0.09	13.94	2.62	-4.10	1.86	3.55	1.76	-0.89	1.93
Darwin	1752.18	3.77	0.81	0.06	-3.46	0.83	-0.04	0.96	-1.94	0.89	-0.60	0.83
East Trout Lake	1796.33	14.22	0.34	0.20	-4.25	2.28	-10.24	2.22	-2.46	2.20	-3.34	2.24
Edwards	1778.30	6.76	0.82	0.10	5.65	1.37	-1.18	1.82	-2.60	1.48	-2.42	1.45
Garmisch	1791.32	4.82	0.52	0.07	0.23	1.13	-7.12	1.10	0.14	1.09	1.64	1.11
Hefei	1832.84	10.16	0.52	0.15	-8.16	2.16	-14.27	2.23	-3.87	2.16	4.57	2.17
Izaña	1767.78	6.62	0.81	0.10	-0.54	1.27	-5.35	1.52	-3.35	1.39	-1.43	1.31
Karlsruhe	1789.08	6.94	0.67	0.11	4.45	1.48	-7.42	1.52	-2.57	1.47	-0.26	1.49
Lamont	1795.05	4.96	0.68	0.07	5.64	1.05	-7.18	1.09	-4.56	1.05	-0.05	1.06
Lauder	1710.82	5.20	0.71	0.08	-5.05	1.10	-2.29	1.14	-1.01	1.10	-1.00	1.11
Ny-Ålesund	1773.64	12.02	0.51	0.14	-8.33	11.38	-17.29	6.87	-7.16	4.14	-3.31	5.96
Orléans	1783.65	8.47	0.71	0.13	8.28	1.86	-7.32	1.88	-0.68	1.86	-0.20	1.83
Paris	1786.57	8.35	0.70	0.13	7.87	1.87	-6.68	2.03	-3.62	1.71	0.67	1.97
Park Falls	1791.76	5.30	0.58	0.08	1.25	1.12	-10.14	1.16	-1.62	1.12	0.58	1.13
Pasadena	1808.84	5.77	0.51	0.09	5.91	1.32	-5.64	1.38	-7.18	1.29	-1.74	1.32
Rikubetsu	1804.65	8.29	0.46	0.13	-9.33	1.76	-14.92	1.82	1.00	1.76	0.31	1.77
Saga	1837.15	6.83	0.32	0.10	-3.19	1.46	-12.60	1.46	-3.43	1.45	1.14	1.45
Sodankylä	1775.84	9.87	0.57	0.15	-4.55	3.23	-11.68	2.17	-1.21	2.50	-1.98	2.39
Tsukuba	1817.98	7.49	0.50	0.11	-2.59	1.66	-10.69	1.80	-1.84	1.69	1.04	1.72
Wollongong	1734.21	5.57	0.66	0.09	-1.38	1.28	-0.09	1.28	1.70	1.27	0.99	1.24

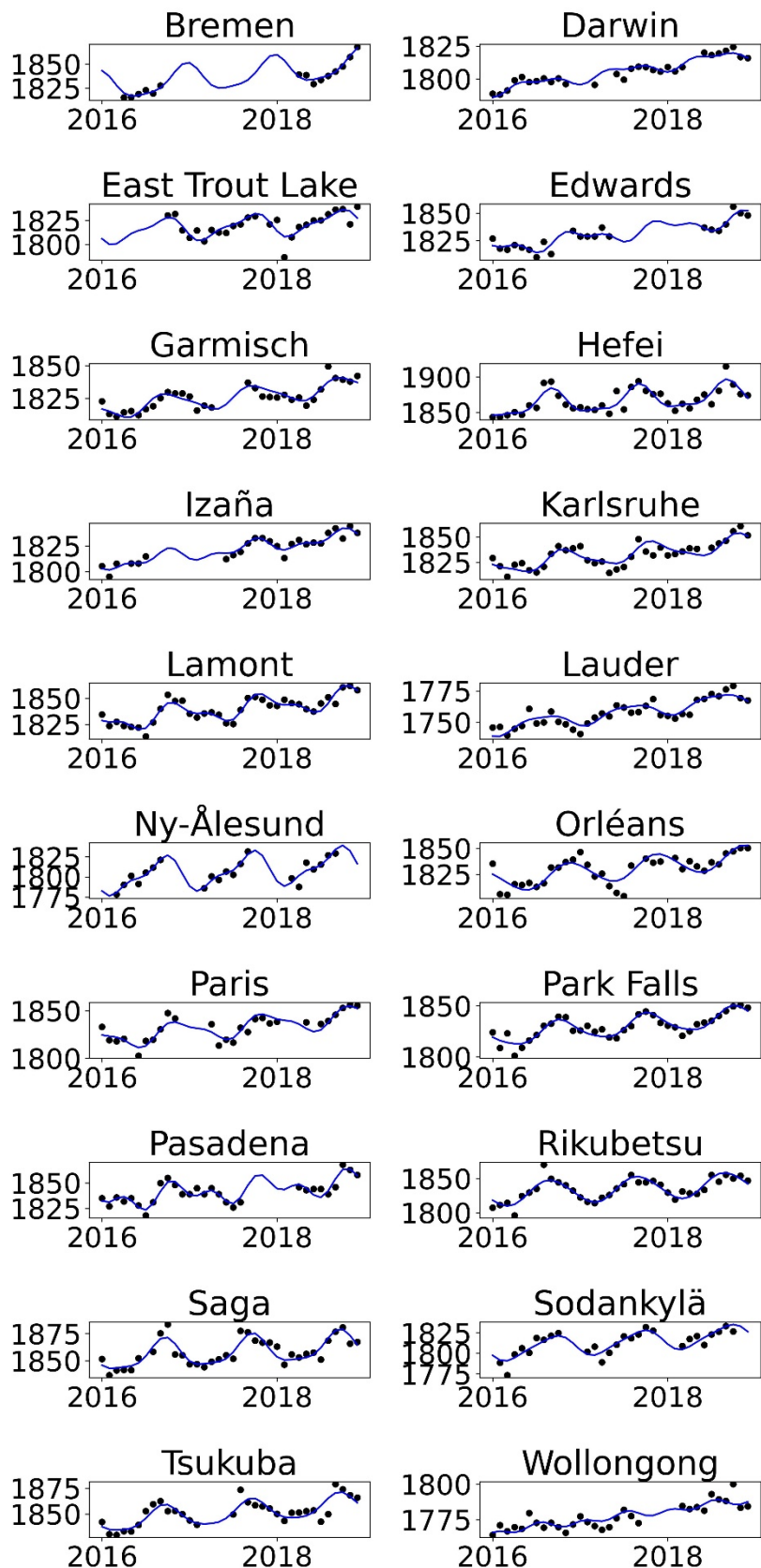


Figure S1. The monthly means of XCH₄ in ppb at each TCCON site analyzed from 2016 to 2019 (black dots) plotted alongside the fitted monthly mean obtained through Fourier regression (blue line). The regression provides a smoothed representation of the underlying seasonal cycle and long-term trends.

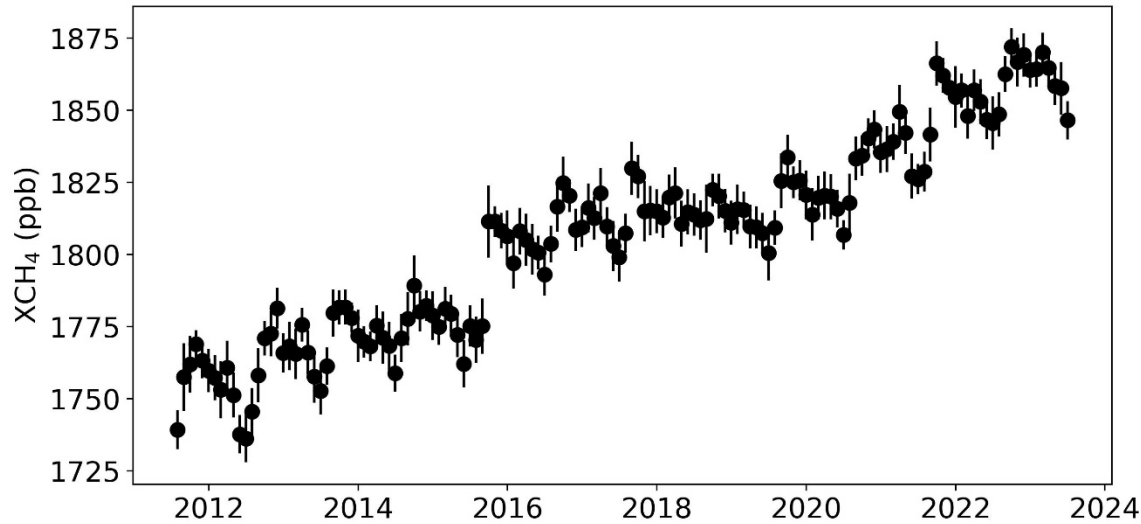


Figure S2. Raw monthly means of XCH₄ measured by CLARS-FTS in the SVO mode from the beginning of the data record in August 2011 to mid-2023. The error bars represent one standard deviation of the mean.

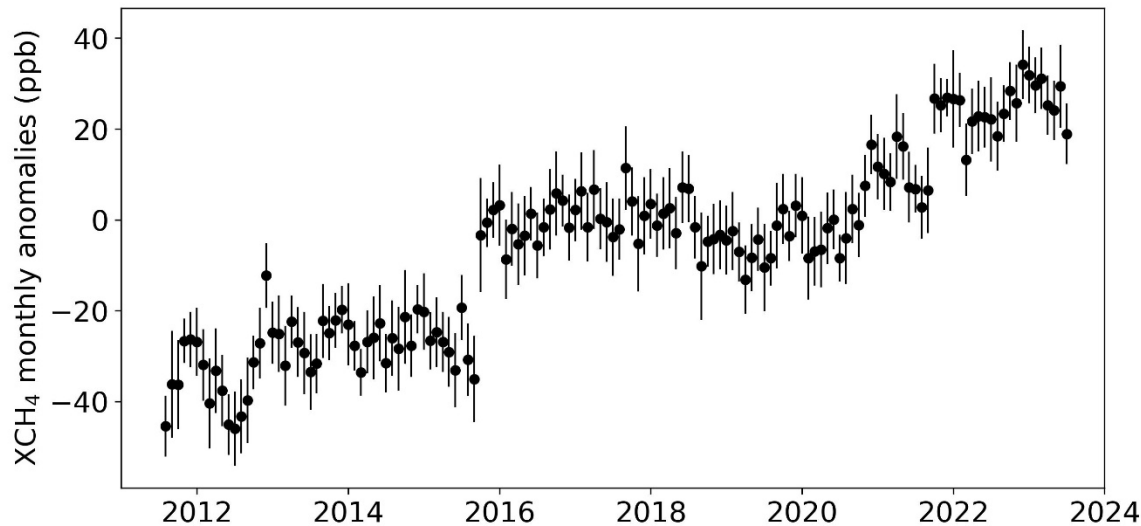


Figure S3. The full deseasonalized and detrended methane time series from CLARS-FTS (SVO mode). The seasonal cycle and a linear trend, derived from 2016-2019 data, have been removed. Error bars represent one standard deviation of the mean.

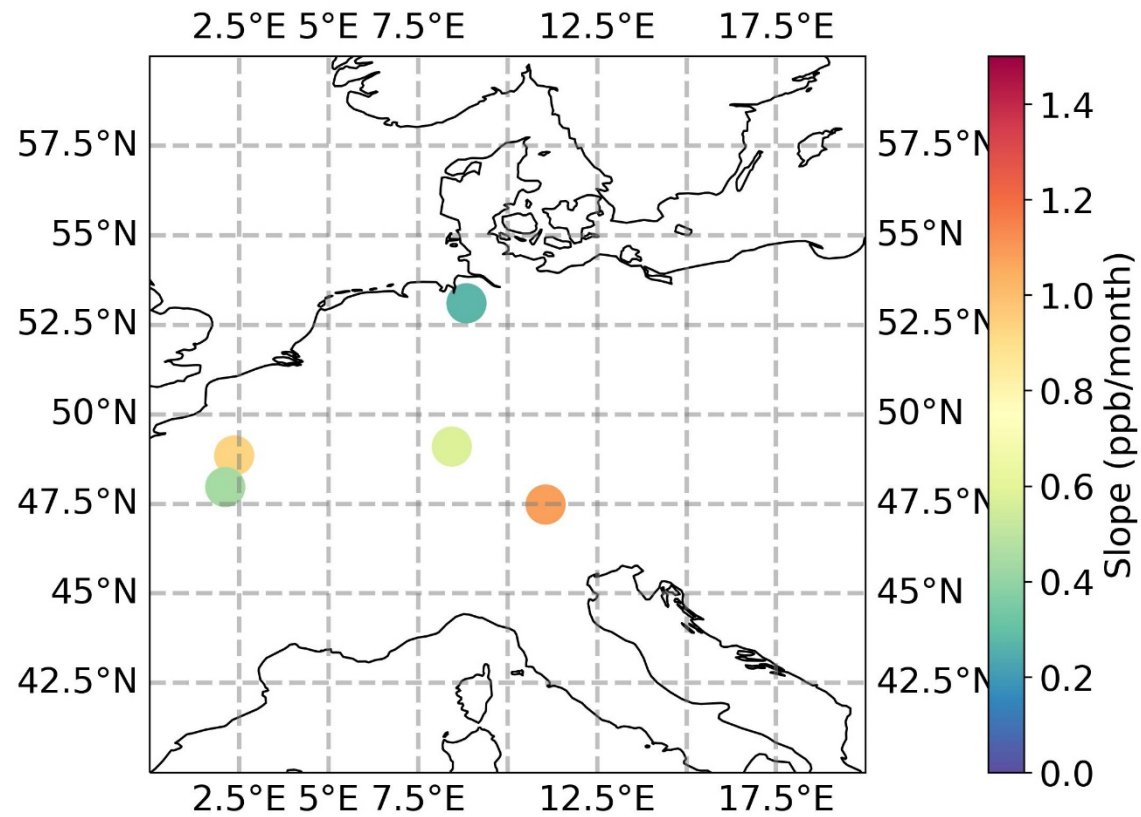


Figure S4. Zoom-in on the methane growth rates observed at the European TCCON sites (Orléans, Paris, Karlsruhe, Bremen, Garmisch) from Figure 5.